

Article

Impact of the ‘Coal-to-Natural Gas’ Policy on Criteria Air Pollutants in Northern China

He Meng¹, Yanjie Shen², Yuan Fang¹ and Yujiao Zhu^{3,*}

¹ Qingdao Eco-Environment Monitoring Center of Shandong Province, Qingdao 266003, China; hemeng.qdemc@gmail.com (H.M.); fy@qd.shandong.cn (Y.F.)

² Laboratory of Marine Environmental Science and Ecology (MoE), Institute for Advanced Ocean Study, Ocean University of China, Qingdao 266100, China; shenyanjie@stu.ouc.edu.cn

³ Environment Research Institute, Shandong University, Qingdao 266237, China

* Correspondence: zhuyujiao@sdu.edu.cn

Abstract: During the last decades, China had issued a series of stringent control measures, resulting in a large decline in air pollutant concentrations. To quantify the net change in air pollutant concentrations driven by emissions, we developed an approach of determining the closed interval of the deweathered percentage change (DPC) in the concentration of air pollutants on an annual scale, as well as the closed intervals of cumulative DPC in a year compared with that in the base year. Thus, the hourly mean mass concentrations of criteria air pollutants to determine their interannual variations and the closed intervals of their DPCs during the heating seasons from 2013 to 2019 in Qingdao (a coastal megacity) were analyzed. The seasonal mean SO₂ concentration decreased from 2013 to 2019. The seasonal mean CO, NO₂, and PM_{2.5} concentrations also generally decreased from 2013 to 2017, but increased unexpectedly in 2018 (from 0.9 mg m⁻³ (CO), 42 μg m⁻³ (NO₂), and 51 μg m⁻³ (PM_{2.5}) in 2017 to 1.1 mg m⁻³, 48 μg m⁻³, and 64 μg m⁻³ in 2018, respectively). The closed intervals of DPC in concentrations of CO, NO₂, and PM_{2.5} from the 2017 heating season (2017/2018) to the 2018 heating season (2018/2019) were obtained at (27%, 30%), (15%, 18%), and (30%, 33%), respectively. Such high positive endpoint values of the closed intervals, in contrast to their small interval lengths, indicate increased emissions of these pollutants and/or their precursors in 2018/2019 compared with 2017/2018, by minimizing the meteorological influences. The rebounds of CO, NO₂, and PM_{2.5} in 2018/2019 were likely associated with a doubled increase in natural gas (NG) consumption implemented by the “coal-to-NG” project, as the total energy consumption showed little difference. Our results suggested an important role of the “coal-to-NG” project in driving concentrations of air pollutant increases in China in 2018/2019, which need integrated assessments.

Keywords: PM_{2.5}; deweathered approach; trend analysis; mitigation effect; natural gas



Citation: Meng, H.; Shen, Y.; Fang, Y.; Zhu, Y. Impact of the ‘Coal-to-Natural Gas’ Policy on Criteria Air Pollutants in Northern China. *Atmosphere* **2022**, *13*, 945. <https://doi.org/10.3390/atmos13060945>

Academic Editor: Antonietta Ianniello

Received: 5 May 2022

Accepted: 6 June 2022

Published: 10 June 2022

Publisher’s Note: MDPI stays neutral with regard to jurisdictional claims in published maps and institutional affiliations.



Copyright: © 2022 by the authors. Licensee MDPI, Basel, Switzerland. This article is an open access article distributed under the terms and conditions of the Creative Commons Attribution (CC BY) license (<https://creativecommons.org/licenses/by/4.0/>).

1. Introduction

China has experienced rapid economic growth and urban expansion in the last four decades, leading to excessive emissions of multiple air pollutants [1–5]. Focus has been placed on severe haze pollution in winter, which is characterized by high mass concentrations of atmospheric particles with an aerodynamic diameter of $\leq 2.5 \mu\text{m}$ (PM_{2.5}) or $\leq 10 \mu\text{m}$ (PM₁₀) [1,3,6]. PM exposure is well-known to cause several adverse health outcomes, such as acute and chronic respiratory illnesses and cardiovascular diseases, or even death, and ambient PM_{2.5} human-health effects have been widely investigated in China [7–9]. For example, it was revealed that a 2.9% increase in household healthcare expenditure was estimated to be attributed to a 1% increase in yearly PM_{2.5} exposure in China [10].

To relieve PM_{2.5} pollution, China has issued a number of stringent control measures since 2013 under the “Action Plan on Prevention and Control of Air Pollution” [11], including the enforcement of flue gas desulfurization and denitrification, elimination of in-use vehicles exhibiting high emissions, implementation of ultralow air pollutant emission

standards, and the implementation of the “coal-to-natural gas (NG)” policy in 2018 across northern China [12,13]. With the implementation of the emission control policies, the overall air quality in China has been significantly improved [2]. The concentrations of PM_{2.5}, PM₁₀, and SO₂ were noticeably decreased, but the still high-level PM and stagnant NO₂ present further challenges [2,11]. Ambient air quality standards in China (GB3095-2012) include six criteria air pollutants: PM_{2.5}, PM₁₀, CO, NO₂, O₃, and SO₂. Air pollutants such as total suspended particulates (TSP), NO_x, Pb, and BaP are listed as other pollutants in GB3095-2012, but their concentrations are not publicly accessible. The Class-1 guide values are 15 µg/m³ (annual) and 35 µg/m³ (daily) for PM_{2.5} concentrations, and 40 µg/m³ (annual) and 50 µg/m³ (daily) for PM₁₀ concentrations, respectively. The four Class-2 guide values are 35 µg/m³, 75 µg/m³, 70 µg/m³, and 150 µg/m³.

NG is commonly considered as a clean fossil fuel, resulting in fewer emissions of air pollutants including primary carbonaceous particles, SO₂, volatile and semi-volatile organic species, etc., than burning coal to produce an equal amount of energy [14,15]. The implementation of the “coal-to-NG” policy is expected to directly reduce air pollutant emissions, and thereby relieve PM_{2.5} air pollution in northern China. Replacing coal with NG for industrial facilities would reduce emissions of SO₂ and PM_{2.5}; however, its impact on NO_x and CO emissions reduction requires further investigation. PM_{2.5} concentrations fluctuated largely with the banned use of solid fuels in Krakow, Poland during the last decades, although a long-term decreasing trend was there [16]. The impact of the “coal-to-NG” program on air quality, especially on criteria pollutants, is contentious; for example, increased concentrations of NO_x and particulate nitrate were reported in Beijing and Tianjin in China in 2018 [12,13]. The impact of this policy on air pollution has not been thoroughly investigated in other parts of northern China because of the lack of air pollutant emission data associated with the program. However, the big challenges associated with the “coal-to-NG” program include: (1) no catalyst available for properly operating for vehicles powered by gasoline and NG; and (2) lack of denitrification facilitates after the replacement. Moreover, the net change in pollution levels after excluding perturbations caused by varying weather conditions is still unknown.

To explore the impact of increased NG consumption on ambient mass concentrations of criteria air pollutants, the influence of varying weather conditions on their interannual variations must first be minimized [17–23]. In the literature, several approaches have been documented to decouple the influence of varying weather conditions from emission-driven changes on the interannual variations in concentrations of air pollutants [19,24–27]. In these approaches, either meteorological and other related parameters or random noises were introduced to estimate the deweathered concentrations of criteria pollutants. However, the uncertainties of the deweathered concentrations were poorly understood. Yao and Zhang proposed an approach to convert the time series of data to concentration series of data so that the perturbation from varying weather conditions can be minimized in assessing the effects of emission reduction on the wet deposition trends of several inorganic ions [21]. Building on this study, we further developed an approach to determine the closed interval of the deweathered percentage change (DPC) in ambient concentrations of criteria pollutants on an annual scale, with the aim of quantifying mitigation effects after minimizing weather impacts on air pollution.

Qingdao is a coastal megacity in northern China that pioneered in the implementation of the “coal-to-NG” program starting in 2018. The annual statistical reports of Qingdao showed that NG consumption almost doubled from 2017 to 2018–2019, and its contribution to the total energy consumption significantly increased from 5% in 2017 to 8–9% in 2018–2019, even though the total energy consumption showed little change in 2017–2019 [28]. Thus, it would be an ideal location for studying the impact of the “coal-to-NG” program on air quality by comparing it with the impact of implemented policies in 2013–2017.

In this study, we focused on interannual changes in PM_{2.5}, PM_{2.5–10} (calculated as PM₁₀ minus PM_{2.5}), CO, NO₂, and SO₂; however, the use of NO_x instead of NO₂ can better

reflect NO_x emissions. We applied the closed intervals of the DPC method to observations in Qingdao during the heating season (from November to the following March) as moderate and heavy air pollution can sometimes occur [17,18,22]. We then rationalized the closed intervals of DPC in concentrations of criteria pollutants in terms of the mitigation measures implemented in different years, with particular attention on the significant increase in NG consumption since 2018. Overall, this study aims at evaluating the effects of the “coal-to-NG” program on air quality by minimizing the perturbation from varying weather conditions. In addition, $\text{PM}_{2.5-10}$ was considered as a coarse particle in this study. Dust storms, dust from unsealed roads, dust from construction and demolition, road traffic, and marine aerosols were usually identified as the major emission sources of coarse particles. Except for dust storms, $\text{PM}_{2.5-10}$ was more related to local emissions rather than long-range transport because of its relatively short residence time in the atmosphere.

2. Materials and Methods

2.1. Study Location

Qingdao is located approximately 500 km from Beijing and Tianjin in northern China (Figure 1). Fourteen air quality monitoring sites, which have been operating since 2013 or earlier and are distributed mainly in urban and semi-urban areas in Qingdao (Figure 1), were chosen to analyze the annual means of air pollutants. All the hourly mean air pollutant concentrations are reported online, such as on IQAir [29], and have been updated every hour in Qingdao since 2013. Hourly mean air pollutant concentrations at the city level were calculated as the mean values of those simultaneously measured at the individual stations. For any hour with missing data in five or more stations, the city-level hourly concentration was also treated as missing data. A total of 3624 (or 3648 in a leap year) hourly data points for each pollutant would be available for one heating season if no data were missing. Approximately 93–94% of the hourly data of the criteria air pollutants for each heating season were available; for example, the number of hourly $\text{PM}_{2.5}$ data ranged from 3372 to 3407 during the heating season from 2013 to 2019.

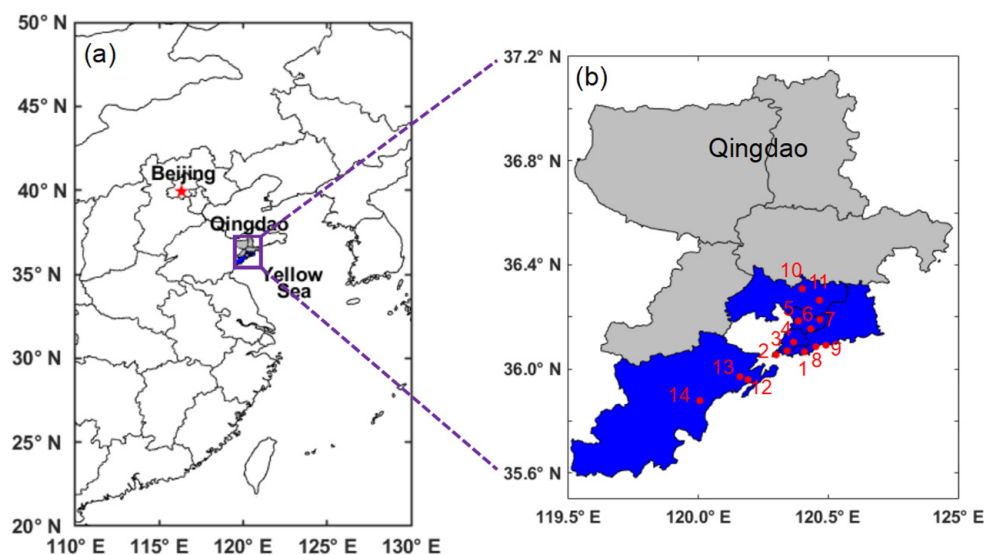


Figure 1. Location of Qingdao (a) and the local network in Qingdao (b) including 14 air quality monitoring sites. Red dots with numbers in figure (b) represent the locations of monitoring stations, and blue and grey areas represent urban and non-urban in Qingdao.

The mitigation measures adopted in Qingdao from 2014 to 2019 are detailed in Tables S1–S3 in Supplementary Materials. The enforcement of flue gas desulfurization and denitrification was implemented primarily in 2014–2015. The adoption of ultralow emission standards began in 2017. High-emission vehicles were eliminated primarily

during 2014–2015. The fines imposed on construction sites that violated local emission control regulations significantly increased in 2017 and 2018. Reports from the State of the Ecology and Environment in Qingdao before 2015 include the total emissions of SO₂ and NO_x, but no emission data have been reported since. The same occurred in other cities in China. This restricts to link variations in the observed concentrations of SO₂ and NO₂ to their emissions.

In addition, air quality in Qingdao has notably improved each year in response to the implementation of various mitigation measures since 2013, which occurred prior to the large increase in NG consumption in 2018. For example, the annual mean mass concentrations of PM_{2.5}, PM₁₀, and SO₂ were 44%, 29%, and 74% lower, respectively, in 2017 than in 2013 [30]. However, the annual mean mass concentrations of PM_{2.5}, PM₁₀, and NO₂ were 9%, 3%, and 3% higher in 2019, respectively, than in 2018 [30].

2.2. Study Period

This study focused on the heating season, which includes November to the following March. The year 2013 was used as the base year, as it is the first year with publicly accessible air quality data; the 2013 heating season (2013/2014) is defined as the period from November 2013 to March 2014. Therefore, the heating seasons from 2014 to 2019 are hereafter referred to as 2014/2015, 2015/2016, 2016/2017, 2017/2018, 2018/2019, and 2019/2020, respectively. Note that two months in 2019/2020 (the period from November 2019 to March 2020), i.e., February and March 2020, were subjected to the COVID-19 lockdown.

2.3. Energy Consumption during Study Period

The consumption of coal, oil, and NG in Qingdao from 2013 to 2020 is shown in Figure S1 in Supplementary Materials, and the data were downloaded from the Qingdao Bureau of Statistics [28]. NG consumption sharply increased from $3.7\text{--}4.5 \times 10^{12}$ kcal in 2013–2017 to $8.5\text{--}9.3 \times 10^{12}$ kcal in 2018–2019 (Figure S1 in Supplementary Materials). Relative to the levels in 2017, coal consumption decreased from 6.9×10^{13} kcal to $6.6\text{--}6.8 \times 10^{13}$ kcal and oil consumption decreased from 3.1×10^{13} kcal to $2.4\text{--}2.7 \times 10^{13}$ kcal in 2018–2019. The total energy consumption narrowly fluctuated around 1×10^{14} kcal between 2014 and 2019, but the contribution of NG consumption to the total energy consumption increased from 4–5% in 2014–2017 to 8–9% in 2018–2019. The total energy consumption in Qingdao decreased to 9.6×10^{13} kcal in 2020 because of the COVID-19 pandemic. During the COVID-19 lockdown period in Qingdao, the total energy consumption and power plant energy consumption decreased by 8–9% and 19–23%, respectively, compared to those of 2019 [28]. The total global energy consumption and air pollutant emissions were reportedly led to a decrease during the COVID-19 lockdown period, based on daily global CO₂ emissions estimates, satellite data, and thousands of ground-level air pollutant observations [31–33]. Thus, we assume that energy consumption in areas neighboring and upwind of Qingdao also decreased in early 2020.

Based on our incomplete survey (no official data in the public domain, personal communication with people managing facilities that adopted “coal-to-NG”), the large increase in NG consumption was mainly attributed to two large chemical facilities (over 80%) to support new production capacity. Less than 20% of the NG consumption increase was attributed to small facilities that were serviced for old production capacities. The national NG consumption in China only increased by approximately 1% per year in 2017, 2018, and 2019 [34].

2.4. Climate Anomalies during Study Period

Meteorological data in Qingdao were downloaded from <http://data.cma.cn/> (assessed on 30 November 2021) with permission after registration. A total of 1200 (or 1208 in a leap year) hourly data for precipitation, wind speed (WS), air temperature (T), and relative humidity (RH) were for one heating season if no data were missing. More than 95% of the data were available for each heating season. The anomalies of climate factors during the

heating seasons were analyzed, with particular attention on the anomalies in 2018/2019 and 2019/2020. Precipitation, WS, T, and RH anomalies during the heating season in each year were calculated relative to the corresponding decade heating seasonal mean in 2010–2019.

The precipitation anomaly from the decade seasonal mean (82 mm in 2010–2019) ranged from -30 mm to 24 mm, except for 123 mm in 2019/2020 (Figure S2a in Supplementary Materials). A much higher precipitation amount was recorded in January and February 2020, which impacted 2019/2020 because of the wet scavenging of air pollutants. The precipitation amount in 2018/2019 was close to the decade seasonal mean, with an anomaly of -8 mm. The wind speed anomaly from the decade seasonal mean of 3.7 m s⁻¹ ranged from -0.3 m s⁻¹ to 0.1 m s⁻¹ (Figure S2b in Supplementary Materials). The minimum anomaly of -0.3 m s⁻¹ occurred in 2018/2019 when the lower wind speeds favored the accumulation of air pollutants and increased their seasonal means to some extent. The seasonal mean wind speed in 2019/2020 was the same as the decade seasonal mean. The ambient temperature anomaly (from the decade seasonal mean of 4 °C) varied from -0.6 °C to $+1.4$ °C (Figure S2c). The maximum anomaly of $+1.4$ °C occurred in 2019/2020, indicating a warmer winter. The anomaly in 2018/2019 was $+0.7$ °C, which was similar to $+0.8$ °C in 2014/2015 and $+0.6$ °C in 2016/2017. Normally, a warm winter is associated with a reduced East Asian winter monsoon [18,20,22], disfavoring the dispersion of air pollutants. However, a large increase in precipitation during 2019/2020 may have overridden the impact of warm winters. The ambient RH anomaly from the decade seasonal mean of 62% varied from -3.1% to 4.4% (Figure S2d in Supplementary Materials). The anomalies were -1.1% and $+4.4\%$ in 2018/2019 and 2019/2020, respectively. Increased ambient RH may accelerate the heterogeneous formation of secondary PM_{2.5} [3,6], while increased precipitation can minimize this impact to some extent.

2.5. Method of Closed Interval of DPCs in Concentrations of Air Pollutants

Unlike the estimation of the deweathered concentrations of criteria air pollutants adopted in the literature [19,24–27], this study alternatively determined the closed interval of the DPC of criteria air pollutant mass concentrations between any two years. To achieve the target, we developed a five-step approach for data processing and analysis because of criteria air pollutant mass concentrations in different years with varying data sizes. Step 1 reconstructed each year's dataset while retaining the original statistical metrics so that each year's dataset was the same size. Step 2 conducted a correlation analysis of the observational data between two consecutive years using the newly constructed datasets from Step 1. The inflection point is visibly identified from the regression curve as the first guess and all data points having a value larger than the inflection point are considered as outliers caused by varying weather conditions or extreme events. Step 3 statistically screened out more outliers by repeating the correlation analysis using the datasets that excluded the outliers identified in Step 2. Step 4 calculated the range of the true DPC between two years, and Step 5 evaluated the residual perturbation, assuming that the impact of varying weather conditions may not be fully excluded from the first four steps. Detailed descriptions of the five steps are provided in the Supplementary Materials. Here, we summarize the key points of each step.

Throughout Steps 1–3, 91–98% of the observational data were left to reconstruct the final arrays for a given pollutant between any two consecutive years of the same size. In Step 4, the linear regression (LR) analysis was repeated for each pair of the final arrays with zero intercept. The LR slope was defined as the primary DPC (DPC_{primary}). Moreover, the LR with a non-zero intercept was conducted using the data in each pair of the final arrays. The LR slope was defined as the secondary DPC (DPC_{secondary}). The R² values of the LR analysis for calculating both DPC_{secondary} and DPC_{primary} or calculating DPC_{secondary} were mostly larger than 0.99, except for a few values larger than 0.96. The true DPC should be theoretically between DPC_{primary} and DPC_{secondary}.

Step 5 evaluated the residual perturbation by varying weather conditions. Theoretically, the intercept in the LR analysis of Step 4 should infinitely approach zero when the

perturbation by varying weather conditions is negligible. This can be clearly identified in approximately 1/3 of the calculated pairs of DPC_{primary} and $DPC_{\text{secondary}}$. Moreover, higher consistency in each pair of DPC_{primary} and $DPC_{\text{secondary}}$ was found for $PM_{2.5}$, the concentrations of which were affected mainly by regional sources [35]. The reverse was generally true for $PM_{2.5-10}$, SO_2 , CO , and NO_2 , whose concentrations were determined largely by local emissions. If $DPC_{\text{secondary}}$ is smaller than DPC_{primary} , the varying weather conditions incompletely removed by Step 3 likely disfavor the accumulation and/or formation of the pollutant. The reverse would be true if $DPC_{\text{secondary}}$ was larger than DPC_{primary} . Thus, DPC_{primary} and $DPC_{\text{secondary}}$ were used to construct the closed interval of DPC in concentrations of criteria pollutants, i.e., $(DPC_{\text{primary}}, DPC_{\text{secondary}})$.

The approach described above was used to determine the closed interval of DPCs in concentrations of all the criteria air pollutants in the years 2014/2015–2019/2020 against those of the base year (2013/2014); the results are shown in Table 1. The DPC can be considered as the cumulative effect of mitigation measures in multiple years and the corresponding interval was hereafter referred to as the closed interval of cumulative DPC in this study.

Table 1. The intervals of DPCs of various pollutants in different years against those in 2013/2014 (%).

Year	$PM_{2.5}$		$PM_{2.5-10}$		SO_2		CO		NO_2	
	DPC_{primary}	$DPC_{\text{secondary}}$								
2014/2015	−19	−20	−20	−12	−33	−31	−3	−4	−14	−4
2015/2016	−17	−11	−21	−30	−44	−48	−1	6	−27	−25
2016/2017	−29	−23	−29	−31	−65	−69	−22	−5	−26	−15
2017/2018	−38	−32	−11	−10	−75	−77	−25	−18	−22	−5
2018/2019	−20	−19	5	10	−79	−80	−5	4	−10	12
2019/2020	−48	−32	−36	−25	−86	−88	−28	−17	−35	−13

There are four advantages of the above-described approach: (1) allowing statistical identification and exclusion of outliers in estimating two endpoints of the closed interval of DPC; (2) confirming the accuracy of DPC when the interval length of DPC is sufficiently small; (3) identifying the large perturbation from varying weather conditions on DPC when the interval length is large; and (4) avoiding direct estimation of deweathered concentrations of air pollutants in which the uncertainties are difficult to accurately evaluate. When the third is the case, the closed intervals can be narrowed simply by combining results extracted from the approaches reported in the literature. Moreover, the links between emissions and ambient concentrations of air pollutants are generally nonlinear. The perturbation from varying weather conditions on ambient concentrations cannot be fully excluded. Thus, the true DPC should always be a closed interval, but not a single value.

3. Results

3.1. Closed Intervals of DPCs in Mass Concentrations of $PM_{2.5}$

The $PM_{2.5}$ seasonal mean concentration varied from $84 \mu\text{g m}^{-3}$ in 2013/2014 to $50 \mu\text{g m}^{-3}$ in 2019/2020. Compared with the previous year, the annual percentage changes in seasonal mean $PM_{2.5}$ were estimated at −19%, −19%, −13%, and −22% in 2014/2015, 2016/2017, 2017/2018, and 2019/2020, respectively, and 6% and 27% in 2015/2016 and 2018/2019, respectively. The negative values in the four years were mostly caused by decreased emissions of $PM_{2.5}$ and/or its precursors [2,11], and partially caused by potential perturbations by varying weather conditions. In contrast, the positive values in 2018/2019 and in 2015/2016 were likely caused by either increased emissions or varying weather conditions. To verify these hypotheses, the closed intervals of DPC in mass concentrations of $PM_{2.5}$ were determined and further discussed.

The hourly mean data of $PM_{2.5}$ concentration reconstructed by Step 1 during the heating season between two consecutive years were plotted in Figure 2a–f. By minimizing the perturbations caused by varying weather conditions, the estimated DPC_{primary} and $DPC_{\text{secondary}}$ of $PM_{2.5}$ from 2013/2014 to 2014/2015 were −19% and −20%, respectively.

The closed interval of DPC was thereby obtained, i.e., (−19%, −20%), with the interval length as low as 1%. Thus, the impact of perturbations caused by varying weather conditions on the estimated DPC were negligible. The differences between DPC_{primary} and $DPC_{\text{secondary}}$ were within 2% for 2014/2015, 2016/2017, 2017/2018, and 2019/2020 compared with those in each previous year, and the values were negative (Figure 3a); however, the DPC_{primary} and $DPC_{\text{secondary}}$ were positive and their differences were slightly larger for 2015/2016 (3% and 8%) and 2018/2019 (30% and 33%), respectively. Note that the difference in $PM_{2.5}$ concentrations between two consecutive years was generally significant ($p < 0.01$), except for 2015/2016 vs. 2014/2015 (Figure 3a).

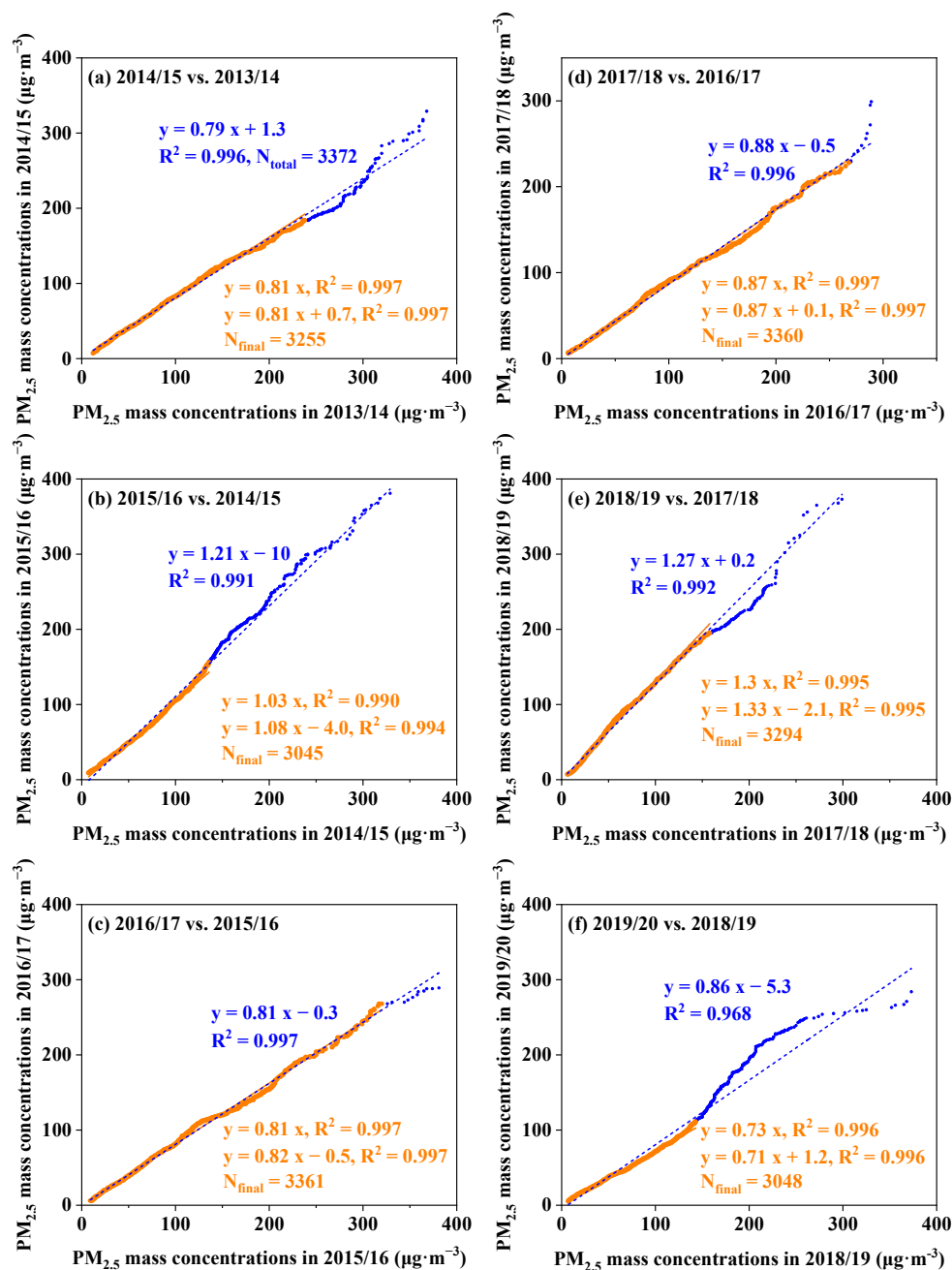


Figure 2. Analysis results of $PM_{2.5}$ mass concentrations in various pairs of arrays reconstructed by Step 1 (a–f) (blue markers and regression curves use all data points, and yellow ones use the selected data by excluding data points that suffered from severe perturbations from the anomalies).

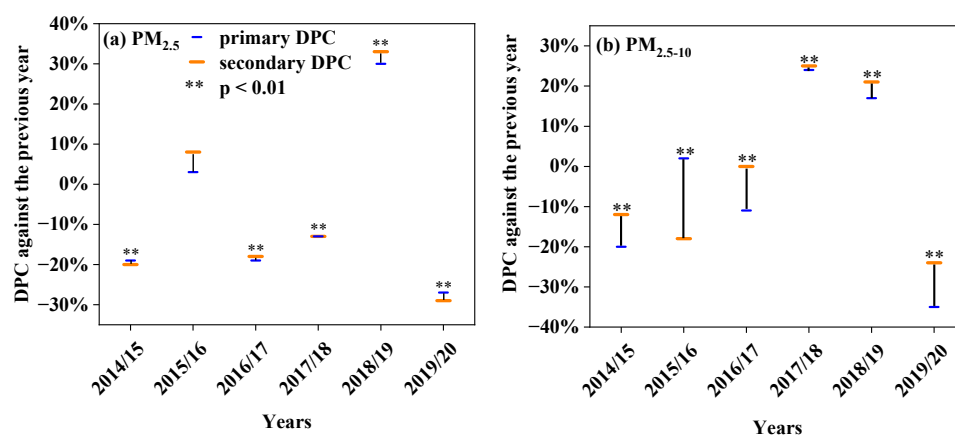


Figure 3. The closed interval of DPCs in PM_{2.5} mass concentrations (a) and PM_{2.5-10} mass concentrations (b). ** refers to statistically significant at $p < 0.01$.

The closed interval of cumulative DPC from 2013/2014 to 2017/2018 was obtained at (−38%, −32%) (Table 1). The closed interval of cumulative DPC from 2013/2014 to 2018/2019 was gained at (−20%, −9%). Although the estimated interval length of cumulative DPCs enlarged to some extent, it was still safe to say that an increase in the latter cumulative DPC compared with the former cumulative DPC was consistent with the positive DPC from 2017/2018 to 2018/2019 (30%, 33%), respectively, and both reflected the emission-driven PM_{2.5} rebound in 2018/2019. However, the closed interval of cumulative DPC from 2013/2014 to 2019/2020 shifted to (−48%, −32%), respectively, which is consistent with the negative DPC from 2018/2019 to 2019/2020 (−27%, −29%), respectively, mentioned above. The COVID-19 lockdown likely caused a large decrease in the emissions of PM_{2.5} and/or its precursors during 2019/2020, consistent with observations globally [31,33]. Clearly, the interval lengths of the cumulative DPCs were larger than any of the aforementioned values for two consecutive years. Investigating the closed intervals of both cumulative DPCs and DPCs in any two consecutive years can solidify the emission-driven increase or decrease in any particular year.

3.2. Closed Intervals of DPCs in PM_{2.5-10}

The invasion of dust storms, which can be easily identified in satellite images and supported by PM_{2.5-10} concentrations of $>150 \mu\text{g m}^{-3}$ combined with a mass PM_{2.5-10} to PM_{2.5} ratio of >2 , usually occurs during the heating season and early spring in northern China [3,17]. Data points with PM_{2.5-10} $>150 \mu\text{g m}^{-3}$ generally deviate from the regression curve to a large extent (Figure 4a–f); these data points were therefore removed from the calculation of the closed interval of DPC because they are unrelated to the mitigation of air pollutants.

Following the same approach used for PM_{2.5}, the estimated endpoint values of the PM_{2.5-10} closed interval of DPC for each year before 2016/2017 were mostly negative compared with those of each previous year (Figure 3b). The closed interval of cumulative DPC from 2013/2014 to 2016/2017 were obtained at (−29%, −31%), respectively (Table 1). There were somewhat large interval lengths of DPC between two consecutive years (e.g., (−20%, −12%) from 2013/2014 to 2014/2015, (+2%, −18%) from 2014/2015 to 2015/2016), suggesting that the incompletely removed perturbation from varying weather conditions largely affected the estimated endpoint values in these years. In contrast, the endpoint values were highly positive from 2016/2017 to 2017/2018 (24%, 25%) and from 2017/2018 to 2018/2019 (17%, 21%), suggesting substantial increases in emission-driven PM_{2.5-10} concentrations. The emission-driven rebound of PM_{2.5-10} in 2017/2018 and 2018/2019 led to the interval of cumulative DPC estimated at (5%, 10%) during the period from 2013/2014 to 2018/2019. Additionally, the closed interval of cumulative DPC from 2013/2014 to 2019/2020 were obtained at (−36%, −25%). The change from the positive cumulative

DPC from 2013/2014 to 2018/2019 to the negative cumulative DPC from 2013/2014 to 2019/2020, and the negative DPC from 2018/2019 to 2019/2020 (−35%, −24%), indicate that the emission-driven $PM_{2.5-10}$ rebound was temporarily halted by the COVID-19 lockdown.

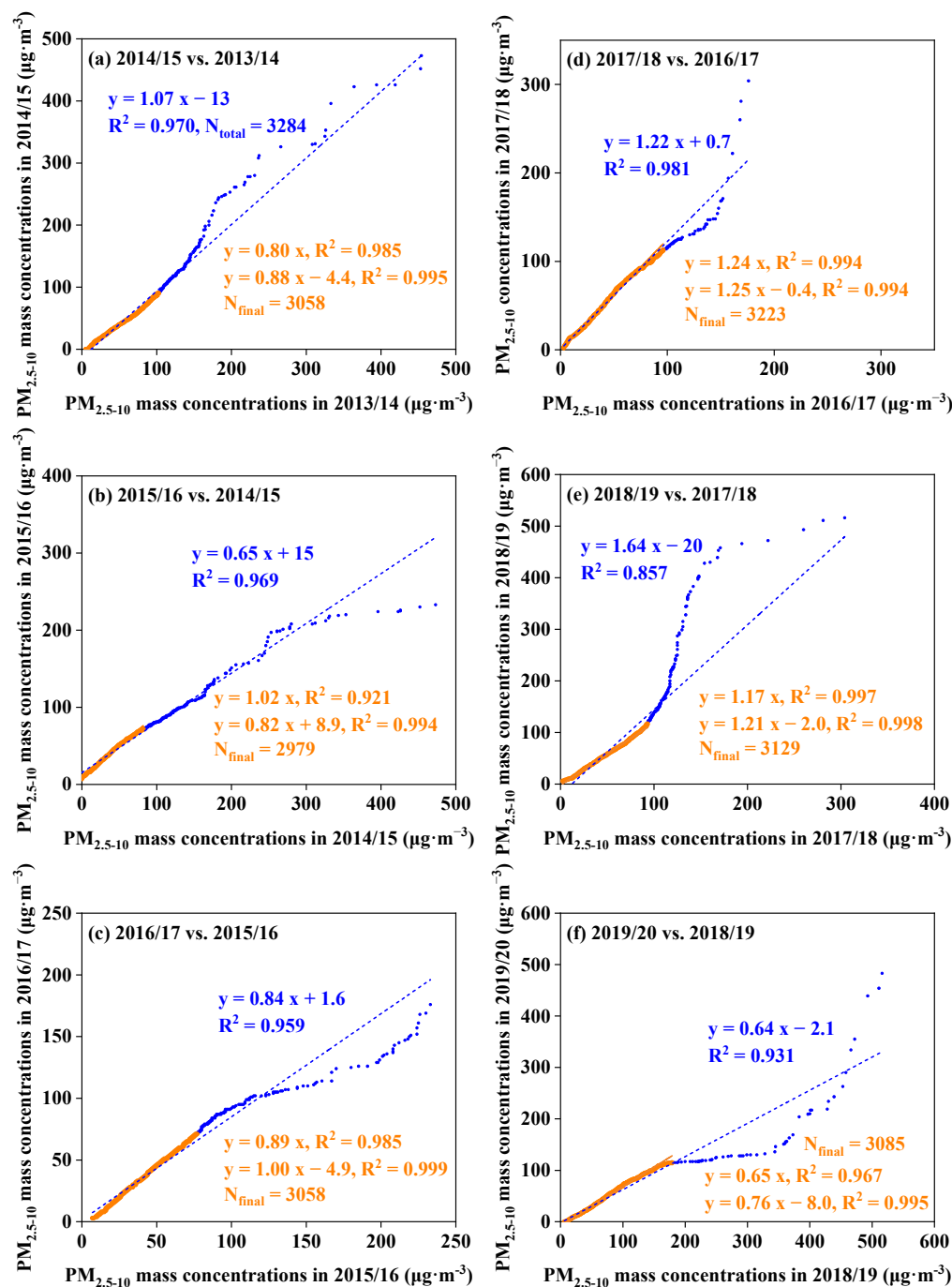


Figure 4. Analysis results of $PM_{2.5-10}$ mass concentrations in various pairs of arrays reconstructed by Step 1 (a–f) (blue markers and regression curves use all data points, and yellow ones use the selected data by excluding data points that suffered from severe perturbations from the anomalies).

3.3. Closed Intervals of DPCs in SO_2 , CO , and NO_2

The estimated DPC in concentrations of SO_2 were always negative compared with those in each previous year, with the largest two endpoint values of −16% and −17% from 2017/2018 to 2018/2019 and the smallest two endpoint values of −35% and −37% from 2015/2016 to 2016/2017 (Figure 5a). The interval length of DPC were mostly less than

2%, except for 8% from 2014/2015 to 2015/2016. The highly negative endpoint values of DPC confirmed annual emission-driven declines in SO₂ concentration from 2013/2014 to 2019/2020, which subsequently led to the close interval of cumulative DPC from 2013/2014 to 2019/2020 at (−86%, −88%) (Table 1).

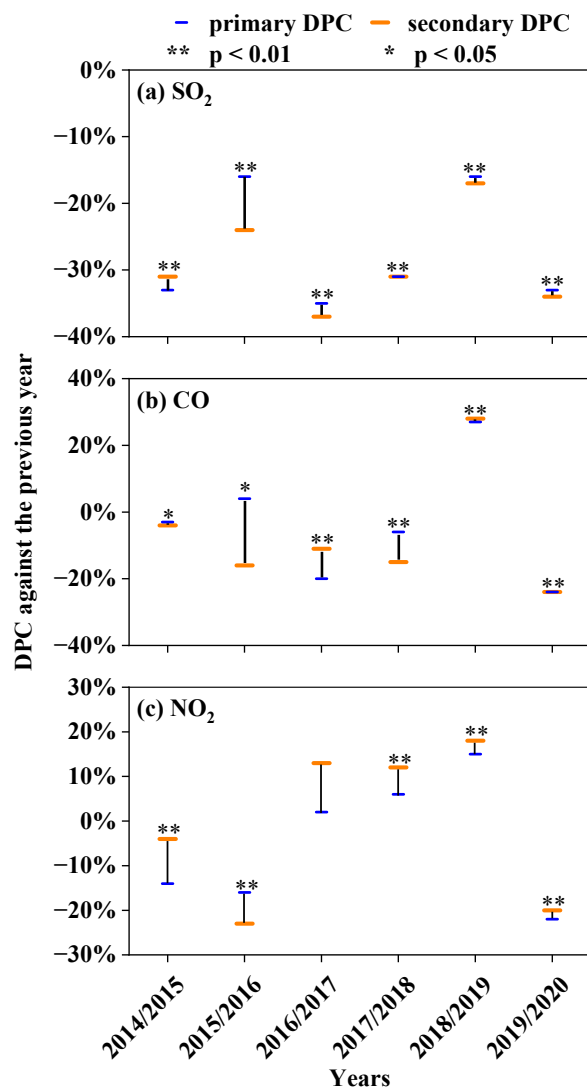


Figure 5. The intervals of DPCs in SO₂ (a), CO (b), and NO₂ (c) in Qingdao from 2014/2015 to 2019/2020. ** refers to statistically significant at $p < 0.01$. * refers to statistically significant at $p < 0.05$.

The estimated DPC in concentrations of CO were also negative compared with those in the previous year, except from 2017/2018 to 2018/2019 (Figure 5b). The intervals of DPC from 2017/2018 to 2018/2019 were, however, at (27%, 30%), indicating a highly positive DPC. The CO pattern is different from that of SO₂ in that an emission-driven rebound of CO concentration prevailed from 2017/2018 to 2018/2019.

The estimated DPCs in NO₂ were negative and the closed intervals at (−14%, −4%) in 2014/2015, (−16%, −23%) in 2015/2016, and (−22%, −20%) in 2019/2020 compared with those of each previous year (Figure 5c). Small-to-medium positive DPC were obtained from 2016/2017 to 2018/2019, with the intervals at (2%, 13%) in 2016/2017, (6%, 12%) in 2017/2018, and (15%, 18%) in 2018/2019 before the COVID-19 pandemic.

4. Discussion

The observed SO₂ in Qingdao was generally derived from local sources associated with industrial sectors, while the SO₂ from long-range transport is typically diluted or

oxidized to a large extent [17,18,33]. The significant negative DPCs in SO₂ throughout the study period are likely due to the local adoption of continuous mitigation measures. NG consumption is commonly regarded as a negligible source of SO₂, and NG replacing coal should therefore decrease SO₂ emissions to some extent. During the COVID-19 lockdown, reduced industrial activities also lowered SO₂ emissions.

The concentrations of CO and NO₂ usually exhibit large spatial variations in Qingdao [29], indicating overwhelming contributions from local sources. The closed interval of cumulative DPC in concentrations of CO from 2013/2014 to 2017/2018 was obtained at (−25%, −18%) (Table 1), which may be due to the overall effect of mitigation measures adopted during 2014–2017. The DPC in CO from 2017/2018 to 2018/2019 suddenly shifted to high positive values at (27%, 30%). Combined with the small interval length (3%), these results imply that increased CO emissions caused a DPC of at least +27%. Such a large increase in DPC from 2017/2018 to 2018/2019 cannot be explained by a 2% decrease in coal consumption and/or a 10% decrease in oil consumption, but rather by an 100% increase in NG consumption. The increased CO emissions from 2017/2018 to 2018/2019 likely negated the reduction in total emissions in 2014/2015–2017/2018, resulting in the closed interval of cumulative DPC at (−5%, 4%) from 2013/2014 to 2018/2019 (Table 1). Again, the COVID-19 lockdown largely reduced the emission of CO, resulting in the closed interval of cumulative DPC at (−28%, −17%) from 2013/2014 to 2019/2020, which was similar to that from 2013/2014 to 2017/2018.

Since 2013, the emission-driven decrease in NO₂ concentrations reportedly occurred across China [36,37]. The closed interval of cumulative DPC in NO₂ from 2013/2014 to 2015/2016 was obtained at (−27%, −25%) (Table 1); this was likely due to the overall effect of mitigation measures adopted in 2014 and 2015, such as eliminating old boilers and high-emission vehicles, and decreasing coal consumption by 15% from 2013 to 2015 (Figure S1a in Supplementary Materials). However, oil consumption increased by 3% from 2015 to 2016 and then decreased by 16% in 2017, while coal consumption only decreased by 1% from 2015 to 2016 and then increased by 9% in 2017. Increased coal consumption was likely the dominant cause of the NO₂ rebound in 2017/2018, leading to the closed interval of cumulative DPC from 2013/2014 to 2017/2018 at (−22%, −5%). Coal and oil consumption decreased by 2% and 10%, respectively, from 2017 to 2018, while the closed interval of DPC was obtained at (15%, 18%) in 2018/2019. Thus, the large increase in NG consumption in 2018 likely caused the emission-driven NO₂ rebound in 2018/2019, further shifting the closed interval of cumulative DPC from 2013/2014 to 2018/2019 to (−10%, 12%). The rebound in 2018/2019 was consistent with a recent report that found that the increased NG consumption in Beijing and Tianjin in northern China may have caused increased concentrations of NO_x and particulate nitrate [13].

Although the DPCs in concentrations of SO₂ and NO₂ were both highly negative (<−16%) from 2014/2015 to 2015/2016, the corresponding DPC in concentration of PM_{2.5} was positive at (3%, 8%). This suggests that, in addition to local sources, long-range transport also contributed significantly to the PM_{2.5} concentration in this city [18,38], particularly because of the longer residence time of PM_{2.5} relative to its gaseous precursors. The exact causes of the unexpected positive DPC of PM_{2.5} in 2015/2016 require further investigation in terms of its chemical composition (e.g., inorganic/organic fractions) and dominant air mass origins, etc. The highly positive DPC of PM_{2.5} from 2017/2018 to 2018/2019 at (30%, 33%) indicates a largely emission-driven rebound in PM_{2.5}, similar to the cases of CO and NO₂, which raises the possibility of increased secondary aerosol formation from increased gaseous precursors at the local scale. Although direct PM_{2.5} emissions from NG combustion should be negligible, incomplete NG combustion may emit organic species with various volatilities [39], which can act as important gaseous precursors of secondary organic aerosols. Further investigation is therefore needed to understand NG emission-related secondary aerosol formation [40]. As newly formed secondary aerosols are mostly fine particles [3,41,42], the above discussion can also partially explain the positive DPC from 2017/2018 to 2018/2019. The DPCs of PM_{2.5–10} were generally negative during

2014/2015–2016/2017, although the interval lengths were relatively large (Figure 3b). The negative DPCs in the first several years were likely due to the overall effects associated with the implemented measures (Tables S1–S3 in Supplementary Materials). In contrast, the positive DPC values in the subsequent two years were likely due to accelerated construction activities (Table S3 in Supplementary Materials), as well as increased local dust emissions. However, the reduced construction activities, on-road vehicle use, and industrial activities because of the COVID-19 lockdown in 2019/2020 changed the DPC to be negative.

5. Conclusions

In this study, we developed a new approach to calculate the closed intervals of DPC in air pollutant concentrations between two consecutive years, as well as the closed intervals of cumulative DPC in a year compared with that in the base year. Thus, the changes in concentrations of air pollutants caused by varying weather conditions were excluded and then the emission-driven changes in concentrations of air pollutants could be studied. The obtained closed intervals indicated that the DPCs extracted before 2018/2019 were generally negative in Qingdao, mainly due to the implementation of mitigation measures. However, the positive DPCs, to be distributed at (27%, 30%) for CO, (15%, 18%) for NO₂, and (30%, 33%) for PM_{2.5} with small interval lengths, from 2017/2018 to 2018/2019 implied emission-driven rebounds of these pollutants rather than changes in meteorological conditions. The comparison between the closed intervals of cumulative DPCs from 2013/2014 to 2018/2019 and those from 2013/2014 to 2017/2018 also supported the analyses. The rebound was likely associated with a doubled increase in NG consumption in 2018, as the total energy consumption showed little difference. By combining our results for Qingdao with previously reported results for the Beijing–Tianjin–Hebei region, we conclude that the “coal-to-NG” program likely caused the increase in NO₂ concentrations on a large scale across northern China. With more official statistics going public, integrated assessments of “coal-to-NG” could be provided.

The obtained closed intervals of DPCs suffered from a broad range in many cases. The interval length was generally even broader for the calculated cumulative DPC. The broad interval length implied that the perturbations caused by varying weather conditions cannot be eliminated. In the cases, a combination of multiple meteorological normalization techniques reported in the literature may be needed to narrow the interval.

Supplementary Materials: The following supporting information can be downloaded at <https://www.mdpi.com/article/10.3390/atmos13060945/s1>: Table S1: Mitigation measures implemented to reduce emissions of air pollutants from coal combustion in Qingdao from 2014 to 2019; Table S2: Mitigation measures implemented to reduce emissions of air pollutants from road dust in Qingdao from 2014 to 2019; Table S3: Mitigation measures implemented to reduce emissions of VOC in Qingdao from 2014 to 2019; Table S4: Statistical comparison between raw array (A₂) and reconstructed array (B₂) for hourly average concentrations of PM_{2.5} in 2014 heating season; Figure S1: Annual coal, oil and natural gas consumption (a) and annual total energy consumption and the percentage of NG in total energy consumption (b) in Qingdao from 2013 to 2020; and Figure S2: Anomalies of precipitation (a), wind speed (b), temperature (c) and relative humidity (d) during the heating seasons in 2013–2019 from their decade seasonal mean in Qingdao.

Author Contributions: Conceptualization, H.M. and Y.Z.; methodology, H.M. and Y.Z.; software, H.M., Y.S. and Y.F.; validation, H.M. and Y.Z.; formal analysis, H.M. and Y.Z.; investigation, H.M. and Y.Z.; resources, H.M., Y.S. and Y.F.; data curation, H.M. and Y.Z.; writing—original draft preparation, H.M. and Y.Z.; writing—review and editing, H.M., Y.S., Y.F. and Y.Z.; visualization, H.M. and Y.Z.; supervision, Y.Z.; project administration, H.M. and Y.Z.; funding acquisition, Y.Z. All authors have read and agreed to the published version of the manuscript.

Funding: This research was supported by the National Natural Science Foundation of China, grant number 42075104, and the Shandong Provincial Natural Science Foundation, grant number ZR2021MD013.

Institutional Review Board Statement: Not applicable.

Informed Consent Statement: Not applicable.

Data Availability Statement: Not applicable.

Acknowledgments: The authors thank Xiaohong Yao for his data processing algorithm.

Conflicts of Interest: The authors declare no conflict of interest.

References

1. An, Z.; Huang, R.-J.; Zhang, R.; Tie, X.; Li, G.; Cao, J.; Zhou, W.; Shi, Z.; Han, Y.; Gu, Z.; et al. Severe haze in northern China: A synergy of anthropogenic emissions and atmospheric processes. *Proc. Natl. Acad. Sci. USA* **2019**, *116*, 8657–8666. [[CrossRef](#)]
2. Cai, S.; Wang, Y.; Zhao, B.; Wang, S.; Chang, X.; Hao, J. The impact of the “Air Pollution Prevention and Control Action Plan” on PM_{2.5} concentrations in Jing-Jin-Ji region during 2012–2020. *Sci. Total Environ.* **2017**, *580*, 197–209. [[CrossRef](#)]
3. Chan, C.K.; Yao, X. Air pollution in mega cities in China. *Atmos. Environ.* **2008**, *42*, 1–42. [[CrossRef](#)]
4. Chang, W.; Zhan, J.; Zhang, Y.; Li, Z.; Xing, J.; Li, J. Emission-driven changes in anthropogenic aerosol concentrations in China during 1970–2010 and its implications for PM_{2.5} control policy. *Atmos. Res.* **2018**, *212*, 106–119. [[CrossRef](#)]
5. Si, Y.; Yu, C.; Zhang, L.; Zhu, W.; Cai, K.; Cheng, L.; Chen, L.; Li, S. Assessment of satellite-estimated near-surface sulfate and nitrate concentrations and their precursor emissions over China from 2006 to 2014. *Sci. Total Environ.* **2019**, *669*, 362–376. [[CrossRef](#)]
6. Ji, D.; Li, L.; Wang, Y.; Zhang, J.; Cheng, M.; Sun, Y.; Liu, Z.; Wang, L.; Tang, G.; Hu, B.; et al. The heaviest particulate air-pollution episodes occurred in northern China in January, 2013: Insights gained from observation. *Atmos. Environ.* **2014**, *92*, 546–556. [[CrossRef](#)]
7. Miller, L.; Xu, X. Ambient PM_{2.5} Human Health Effects—Findings in China and Research Directions. *Atmosphere* **2018**, *9*, 424. [[CrossRef](#)]
8. Lu, X.; Lin, C.; Li, W.; Chen, Y.; Huang, Y.; Fung, J.C.; Lau, A.K. Analysis of the adverse health effects of PM_{2.5} from 2001 to 2017 in China and the role of urbanization in aggravating the health burden. *Sci. Total Environ.* **2019**, *652*, 683–695. [[CrossRef](#)]
9. Wang, Y.; Wild, O.; Chen, H.; Gao, M.; Wu, Q.; Qi, Y.; Chen, X.; Wang, Z. Acute and chronic health impacts of PM_{2.5} in China and the influence of interannual meteorological variability. *Atmos. Environ.* **2020**, *229*, 117397. [[CrossRef](#)]
10. Yang, J.; Zhang, B. Air pollution and healthcare expenditure: Implication for the benefit of air pollution control in China. *Environ. Int.* **2018**, *120*, 443–455. [[CrossRef](#)]
11. Wang, J.; Zhao, B.; Wang, S.; Yang, F.; Xing, J.; Morawska, L.; Ding, A.; Kulmala, M.; Kerminen, V.-M.; Kujansuu, J.; et al. Particulate matter pollution over China and the effects of control policies. *Sci. Total Environ.* **2017**, *584–585*, 426–447. [[CrossRef](#)]
12. Feng, X.; Li, Q.; Tao, Y.; Ding, S.; Chen, Y.; Li, X.-D. Impact of Coal Replacing Project on atmospheric fine aerosol nitrate loading and formation pathways in urban Tianjin: Insights from chemical composition and ¹⁵N and ¹⁸O isotope ratios. *Sci. Total Environ.* **2020**, *708*, 134797. [[CrossRef](#)]
13. Zhao, S.; Hu, B.; Gao, W.; Li, L.; Huang, W.; Wang, L.; Yang, Y.; Liu, J.; Li, J.; Ji, D.; et al. Effect of the “coal to gas” project on atmospheric NO_x during the heating period at a suburban site between Beijing and Tianjin. *Atmos. Res.* **2020**, *241*, 104977. [[CrossRef](#)]
14. Bassano, C.; Deiana, P.; Vilardi, G.; Verdone, N. Modeling and economic evaluation of carbon capture and storage technologies integrated into synthetic natural gas and power-to-gas plants. *Appl. Energy* **2020**, *263*, 114590. [[CrossRef](#)]
15. Rispoli, A.L.; Iaquaniello, G.; Salladini, A.; Verdone, N.; Pepe, M.R.; Borgogna, A.; Vilardi, G. Simultaneous decarbonisation of steel and Oil&Gas industry by MSW gasification: Economic and environmental analysis. *Energy Convers. Manag.* **2021**, *245*, 114577. [[CrossRef](#)]
16. Danek, T.; Zareba, M. The Use of Public Data from Low-Cost Sensors for the Geospatial Analysis of Air Pollution from Solid Fuel Heating during the COVID-19 Pandemic Spring Period in Krakow, Poland. *Sensors* **2021**, *21*, 5208. [[CrossRef](#)]
17. Gao, H.; Chen, J.; Wang, B.; Tan, S.-C.; Lee, C.M.; Yao, X.; Yan, H.; Shi, J. A study of air pollution of city clusters. *Atmos. Environ.* **2011**, *45*, 3069–3077. [[CrossRef](#)]
18. Gao, Y.; Shan, H.; Zhang, S.; Sheng, L.; Li, J.; Zhang, J.; Ma, M.; Meng, H.; Luo, K.; Gao, H.; et al. Characteristics and sources of PM_{2.5} with focus on two severe pollution events in a coastal city of Qingdao, China. *Chemosphere* **2020**, *247*, 125861. [[CrossRef](#)]
19. Grange, S.K.; Carslaw, D.C. Using meteorological normalisation to detect interventions in air quality time series. *Sci. Total Environ.* **2019**, *653*, 578–588. [[CrossRef](#)]
20. Xu, Y.; Xue, W.; Lei, Y.; Huang, Q.; Zhao, Y.; Cheng, S.; Ren, Z.; Wang, J. Spatiotemporal variation in the impact of meteorological conditions on PM_{2.5} pollution in China from 2000 to 2017. *Atmos. Environ.* **2020**, *223*, 117215. [[CrossRef](#)]
21. Yao, X.; Zhang, L. Decoding long-term trends in the wet deposition of sulfate, nitrate, and ammonium after reducing the perturbation from climate anomalies. *Atmos. Chem. Phys.* **2020**, *20*, 721–733. [[CrossRef](#)]
22. Shen, Y.; Meng, H.; Yao, X.; Peng, Z.; Sun, Y.; Zhang, J.; Gao, Y.; Feng, L.; Liu, X.; Gao, H. Does Ambient Secondary Conversion or the Prolonged Fast Conversion in Combustion Plumes Cause Severe PM_{2.5} Air Pollution in China? *Atmosphere* **2022**, *13*, 673. [[CrossRef](#)]

23. Zhang, Y.; Van Vu, T.; Sun, J.; He, J.; Shen, X.; Lin, W.; Zhang, X.; Zhong, J.; Gao, W.; Wang, Y.; et al. Significant Changes in Chemistry of Fine Particles in Wintertime Beijing from 2007 to 2017: Impact of Clean Air Actions. *Environ. Sci. Technol.* **2020**, *54*, 1344–1352. [[CrossRef](#)]
24. Carslaw, D.C.; Taylor, P.J. Analysis of air pollution data at a mixed source location using boosted regression trees. *Atmos. Environ.* **2009**, *43*, 3563–3570. [[CrossRef](#)]
25. Fu, H.; Zhang, Y.; Liao, C.; Mao, L.; Wang, Z.; Hong, N. Investigating PM_{2.5} responses to other air pollutants and meteorological factors across multiple temporal scales. *Sci. Rep.* **2020**, *10*, 15639. [[CrossRef](#)]
26. Dang, R.; Liao, H.; Fu, Y. Quantifying the anthropogenic and meteorological influences on summertime surface ozone in China over 2012–2017. *Sci. Total Environ.* **2021**, *754*, 142394. [[CrossRef](#)]
27. Gong, S.; Liu, H.; Zhang, B.; He, J.; Zhang, H.; Wang, Y.; Wang, S.; Zhang, L.; Wang, J. Assessment of meteorology vs. control measures in the China fine particular matter trend from 2013 to 2019 by an environmental meteorology index. *Atmos. Chem. Phys.* **2021**, *21*, 2999–3013. [[CrossRef](#)]
28. Qingdao Statistical Yearbook 2017, 2018, 2019, 2020. Available online: http://qdtj.qingdao.gov.cn/tongjisj/tjsj_tjgb/ (accessed on 30 November 2021).
29. IQAir. Air Quality in Qingdao. Available online: <https://www.iqair.com/china/shandong/qingdao> (accessed on 30 November 2021).
30. Report on the State of the Ecology and Environment in Qingdao 2013, 2017, 2018, 2019. Available online: <http://mbee.qingdao.gov.cn/n28356059/index.html> (accessed on 30 November 2021).
31. Diamond, M.S.; Wood, R. Limited Regional Aerosol and Cloud Microphysical Changes Despite Unprecedented Decline in Nitrogen Oxide Pollution During the February 2020 COVID-19 Shutdown in China. *Geophys. Res. Lett.* **2020**, *47*, e2020GL088913. [[CrossRef](#)]
32. Le Quéré, C.; Jackson, R.B.; Jones, M.W.; Smith, A.; Abernethy, S.; Andrew, R.M.; De-Gol, A.J.; Willis, D.R.; Shan, Y.; Canadell, J.G.; et al. Temporary reduction in daily global CO₂ emissions during the COVID-19 forced confinement. *Nat. Clim. Chang.* **2020**, *10*, 647–653. [[CrossRef](#)]
33. Venter, Z.S.; Aunan, K.; Chowdhury, S.; Lelieveld, J. COVID-19 lockdowns cause global air pollution declines. *Proc. Natl. Acad. Sci. USA* **2020**, *117*, 18984–18990. [[CrossRef](#)]
34. National Statistical Yearbook of China 2017, 2018, 2019. Available online: <http://www.stats.gov.cn/tjsj/ndsj/> (accessed on 30 November 2021).
35. Liu, X.; Chang, M.; Zhang, J.; Wang, J.; Gao, H.; Gao, Y.; Yao, X. Rethinking the causes of extreme heavy winter PM_{2.5} pollution events in northern China. *Sci. Total Environ.* **2021**, *794*, 148637. [[CrossRef](#)]
36. Li, K.; Jacob, D.J.; Liao, H.; Shen, L.; Zhang, Q.; Bates, K.H. Anthropogenic drivers of 2013–2017 trends in summer surface ozone in China. *Proc. Natl. Acad. Sci. USA* **2019**, *116*, 422–427. [[CrossRef](#)]
37. Lin, C.; Lau, A.K.; Fung, J.C.; Song, Y.; Li, Y.; Tao, M.; Lu, X.; Ma, J.; Lao, X.Q. Removing the effects of meteorological factors on changes in nitrogen dioxide and ozone concentrations in China from 2013 to 2020. *Sci. Total Environ.* **2021**, *793*, 148575. [[CrossRef](#)]
38. Li, K.; Zhu, Y.; Gao, H.; Yao, X. A comparative study of cloud condensation nuclei measured between non-heating and heating periods at a suburb site of Qingdao in the North China. *Atmos. Environ.* **2015**, *112*, 40–53. [[CrossRef](#)]
39. Giani, P.; Balzarini, A.; Pirovano, G.; Gilardoni, S.; Paglione, M.; Colombi, C.; Gianelle, V.L.; Belis, C.A.; Poluzzi, V.; Lonati, G. Influence of semi- and intermediate-volatile organic compounds (S/IVOC) parameterizations, volatility distributions and aging schemes on organic aerosol modelling in winter conditions. *Atmos. Environ.* **2019**, *213*, 11–24. [[CrossRef](#)]
40. Xing, M.; Liu, W.; Li, X.; Zhou, W.; Wang, Q.; Tian, J.; Li, X.; Tie, X.; Li, G.; Cao, J.; et al. Vapor isotopic evidence for the worsening of winter air quality by anthropogenic combustion-derived water. *Proc. Natl. Acad. Sci. USA* **2020**, *117*, 33005–33010. [[CrossRef](#)] [[PubMed](#)]
41. Man, H.; Zhu, Y.; Ji, F.; Yao, X.; Lau, N.T.; Li, Y.; Lee, B.P.; Chan, C.K. Comparison of Daytime and Nighttime New Particle Growth at the HKUST Supersite in Hong Kong. *Environ. Sci. Technol.* **2015**, *49*, 7170–7178. [[CrossRef](#)]
42. Zhu, Y.; Sabaliauskas, K.; Liu, X.; Meng, H.; Gao, H.; Jeong, C.-H.; Evans, G.J.; Yao, X. Comparative analysis of new particle formation events in less and severely polluted urban atmosphere. *Atmos. Environ.* **2014**, *98*, 655–664. [[CrossRef](#)]